An X-ray photoelectron spectroscopy investigation of chromium conversion coatings and chromium compounds

R. Chapaneri[1], G.W. Critchlow[1], I. Sutherland[1],G.D. Wilcox[1],
A. Chojnicki[2], T. Pearson[2] and A.J. Rowan[2]
G. Beamson[3]

[1] *Institute of Polymer Technology and Materials Engineering, Loughborough University, Leicestershire. LE11 3TU. UK. R.Chapaneri@lboro.ac.uk*
[2]*MacDermid plc, Birmingham, West Midlands. B9 4EU. UK.*
[3]*National Centre for Electron Spectroscopy and Surface Analysis (NCESS), STFC Daresbury Laboratory, Warrington, Cheshire, WA4 4AD. UK.*

Summary

Hexavalent and trivalent chromium based conversion coatings on zinc electrodeposited steel have been investigated using X-ray photoelectron spectroscopy (XPS) with the aim of elucidating their film chemistry. Furthermore, a monochromatic Al Kα X-ray source was utilised and the spectra produced evaluated using curve fitting software to elucidate oxidation state information. In addition, a number of chromium compounds were investigated and used to complement the curve fitting analysis for the conversion coatings.

High resolution Cr2p spectra from chromium compounds exhibited multiplet splitting for Cr_2O_3. Additional satellite emissions can also be observed for Cr_2O_3 and $Cr(OH)_3$. Curve fitting of hexavalent chromium conversion coating (CCC) $2p_{3/2}$ spectra contained both Cr(VI) and Cr(III) species with the content of the former slightly higher when the X-ray beam take-off angle (TOA) was reduced to determine more surface specific information. The Cr(III) content was determined to be mainly composed of $Cr(OH)_3$ with some Cr_2O_3. In comparison, trivalent CCCs were largely composed of Cr_2O_3 as opposed to $Cr(OH)_3$. Survey scans of both coatings revealed that the trivalent CCCs had a higher relative zinc content.

Introduction

Chromium based treatment solutions are a favoured choice within industry for the conversion coating of electrodeposited zinc and zinc alloy based coatings. The basis of these coatings is a mixed metal oxide composition formed as a result of anodic / cathodic reactions between the treatment solution and substrate [1]. X-ray photoelectron spectroscopy (XPS) has played a significant role in providing surface chemical compositions and, importantly, oxidation state information for such coatings. Previous investigations, particularly those based on hexavalent chromium coating chemistry, utilised high resolution XPS scans via a non-monochromatic Al/Mg Kα X-ray source [2-6]. However, monochromatic Al/Mg Kα sources offer improved spectral resolution, signal-to-noise ratio as well as a reduced influence of spectral background features such as Bremstrahlung radiation and X-ray satellites. This has enabled previous researchers to take into account additional spectral structure such as multiplet spitting [7,8] and satellite emissions [8] of chromium compounds such as Cr_2O_3. Importantly, utilisation of a monochromatic Al Kα source allows for a less ambiguous determination of the relative concentrations of the different surface

oxidation states. Such information is important in order to understand the deposition mechanisms and functionality of conversion coatings.
In this investigation a standard hexavalent chromium conversion coating (CCC) on zinc electrodeposited steel has been analysed and compared to a commercial trivalent chromium conversion coating (CCC) using a monochromatic Al Kα X-ray source. A collection of reference chromium compounds, namely; Cr_2O_3, CrO_3 and $Cr(OH)_3$ have been analysed and then used as templates for the curve fitting of high resolution coating spectra. By obtaining more accurate peak shapes from curve fitting of reference chromium compound structures such as multiplet splitting, a more accurate estimate can be made for the Cr(III) and Cr(VI) contents within the coatings. Near surface depth profiling was also carried out on hexavalent CCCs via incident X-ray beam take-off angle (TOA) variation.

Experimental

Sample preparation
Chromium(VI) oxide (CrO_3) 99.99% standard was obtained from Sigma Aldrich, chromium(III) oxide (Cr_2O_3) 99.9% was obtained from Fisher Scientific. Chromium hydroxide ($Cr(OH)_3$) was obtained via precipitation [7] of hydrous chromium chloride (1M) with ammonia solution (0.1M). All chromium compounds were obtained in a powder form and placed onto double sided adhesive tape (10mm diameter), mounted on a stainless steel stub. In an effort to alleviate atmospheric contamination specimens were immediately transferred to the spectrometer following loading.

The trivalent CCC treatment was a commercial formulation. The formulation of the hexavalent CCC treatment is provided below (see table 1). An immersion time of 20 seconds and pH of 1.8 were used. Both treatment solutions were applied onto zinc electrodeposited (8µm nominal coating thickness) polished mild steel panels with a resulting CCC thickness of 105-140 nm. Coating thicknesses were obtained from freeze fracture secondary electron microscopy (SEM) studies.

Table 1 – Hexavalent chromium conversion coating formulation

Chemical	**g/l**
Chromic acid (H_2CrO_4)	0.72
Sodium dichromate ($Na_2Cr_2O_7$ $2H_2O$)	0.64
Sulphuric acid (77%) (H_2SO_4)	0.16
Nitric acid (59%) (HNO_3)	1.17

XPS analysis
XPS was carried out using a SCIENTA ESCA300 spectrometer, interfaced with a monochromatic Al Kα X-ray excited sources (1486.6 eV). The electron take-off-angle (measured relative to the sample surface) was set to 90° for the majority of the investigation with 10° and 30° used in specific cases for depth profiling of the uppermost surface regions. A pass energy of 150 eV and an analyser slit width of 0.8 mm were used for both survey and high resolution Al Kα scans. Al Kα X-ray source anode voltage was set at 14 kV, with a filament current of 200 mA. Region spectra were recorded with a step interval of 0.05 eV, a step time of 0.1 sec/scan and with co-addition of 5 to 10 scans.

The spectrometer energy scale was checked regularly using the Fermi edge, $3d_{5/2}$ and M_4VV lines of a sputter cleaned sample of Ag foil. The measured binding

energies came within 0.1 eV of the corresponding literature values (0.0, 368.26 and 1128.78 eV respectively).

The XPS spectrometer was also equipped with a thermoionic emission electron flood gun which was used to facilitate charge compensation. Charge compensation was achieved using a low energy electron flood gun (Scienta FG300) with the gun settings adjusted for optimal spectral resolution.

Elemental quantification from survey scans was achieved using theoretically derived relative sensitivity factors and measuring element peak areas (e.g. 1s, 2p) following subtraction of a Shirley type background. This was carried out using ESCA300 DOS software (version 1.29) [9].

High resolution scans were analysed using XPSPEAK version 4.1 curve fitting software [10] based on a Gaussian-Lorentzian function. To subtract additional line information a Shirley type background was fitted to each spectrum. In the case of Cr2p spectra the background was only fitted to the $2p_{3/2}$ peak component. This peak has a greater intensity for evaluating features such as multiplet splitting in comparison to the $2p_{1/2}$ peak.

In order to obtain fitting parameters for the curves generated on hexavalent and trivalent CCCs, the peak envelopes from the chromium standards (Cr_2O_3, CrO_3, and $Cr(OH)_3$) were initially analysed. It is important to note that the number of peaks assigned to the envelopes on each standard was dependent upon the number of inflections physically observed in the $Cr2p_{3/2}$ spectra. Their resulting parameters such as peak maximum binding energy value, full width at half maximum (FWHM) and peak area were then fixed according to the data and constrained to the major peak within the standard. Only the peak area of the major peak was allowed to change during fitting with all other minor peaks constrained around it. In the case of O1s spectra, curve fitting peaks were added in relation to the number of shoulders physically observed. Respective O1s peak envelopes for chromium standards were not used as fitting parameters for the curve fitting of chromium coatings, which was used in the case of Cr2p data.

All derived peak maximum binding energy values were charge referenced to the main adventitious carbon peak of 285 eV.

Results

Reference chromium compound survey scans

Survey scan results for the reference compounds are provided in table 2. Using atomic percentage values it is possible to calculate the ratio of Cr to O and compare this to the nominal compound ratio. The $Cr(OH)_3$, CrO_3 and Cr_2O_3 ratios are very much in line with expected values. It is important to note that CrO_3 and Cr_2O_3 chromium ratios may also be influenced by small levels of reduction and oxidation of chromium. For $Cr(OH)_3$, some of the additional oxygen may be associated with water strongly absorbed as opposed to vapourised under vacuum and X-ray beam exposure.

Table 2 – Survey scan atomic percentage data of reference chromium compounds

	Atomic %				Chromium Ratio
	C1s	O1s	Cr2p	Cl2p	O:Cr
CrO_3	15.1	60.4	24.5	0.0	2.5
Cr_2O_3	13.7	53.9	32.4	0.0	1.7
$Cr(OH)_3$	30.3	51.8	15.6	2.3	3.3

Chromium (III) oxide (Cr_2O_3)

A high resolution Cr_2O_3 Cr2p spectrum is provided in figure 1a. The spectrum resembles the profile observed by Biesinger et al [7], Unveren et al [8] and Ilton et al [11]. Multiplet splitting is clearly evident on the $2p_{3/2}$ profile as is a $2p_{1/2}$ satellite located around 597 eV. The corresponding $2p_{3/2}$ satellite may be overlapped by the Cr $2p_{1/2}$ profile. The $2p_{3/2}$ profile was fitted with four peaks in correspondence with distinct shoulders in the spectrum profile. A high resolution Cr_2O_3 O1s spectrum is provided in figure 1b. A major sharp peak and shoulder is observed at around 530.45 and 531.56 eV respectively (table 4).

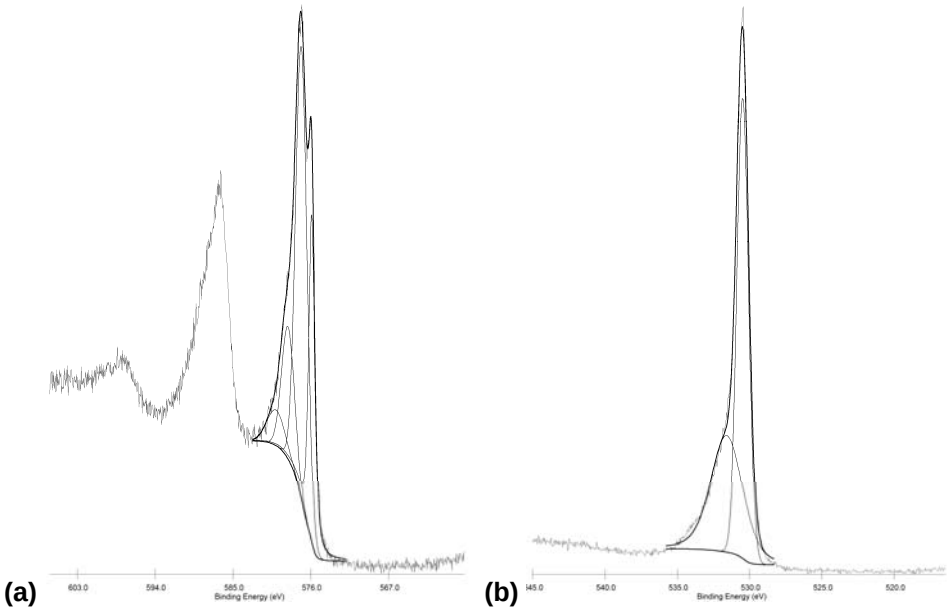

Figure 1 - High resolution Cr2p (a) O1s (b) spectra of Cr_2O_3 compound

Chromium (VI) oxide (CrO_3)

A high resolution CrO_3 Cr2p spectrum is provided in figure 2a. The profile again is similar to a Cr(VI) spectrum profile observed by Biesinger et al [7]. The main peak maximum of 579.96 eV from the $2p_{3/2}$ spectrum is, however, higher than that given by Biesinger et al. for a $PbCrO_4$ crocoite compound (578.9 eV) and the average value based on National Institute of Standards and Technology (NIST) XPS database for Cr(VI) compounds (579.5 eV) [7,12]. It is important to note that although the chromium compounds referred to may be similar in oxidation state to that used in this investigation, their respective chemical environment i.e. groups present in different compounds could also contribute towards slightly different binding energy values.

The Cr $2p_{3/2}$ profile does not show evidence of multiplet splitting, or additional satellite structures. Additional peaks either side of the main $2p_{3/2}$ maximum peak may be due to reduction under vacuum and/or X-ray beam exposure of Cr(VI) [6,13,14],

compound impurities or background contributions. Using the peak maximum binding energy (BE) values 578.30 and 581.06 eV from curve fitting data (table 3) it may be possible to ascribe $Cr(OH)_3$ to the former, whilst the latter could be associated with a compound impurity or background contribution.

A high resolution CrO_3 O1s spectrum is provided in figure 2b. The profile is similar to that observed for Cr_2O_3 (see figure 1b), however, the shoulder is less pronounced and is reflected by its reduced relative peak area (table 4). The binding energy values for the main and shoulder peaks in comparison to Cr_2O_3 are ~0.3 eV higher.

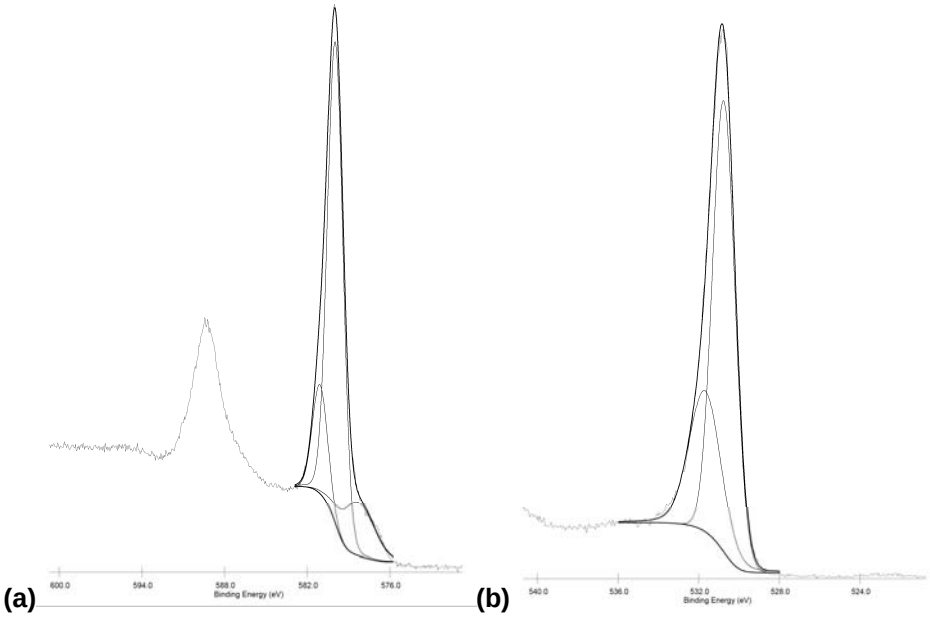

Figure 2 – High resolution Cr2p (a) O1s (b) spectra of CrO_3 compound

Chromium hydroxide $Cr(OH)_3$

A high resolution $Cr(OH)_3$ Cr2p spectrum is provided in figure 3a. The $2p_{3/2}$ peak maximum binding energy value was established as 577.79 eV (see table 4). This, in comparison to binding energy values listed by other researchers, is high (c.f. 577.3 eV [6,7]. It could be suggested that the higher binding energy value is a function of the remaining $CrCl_3$ from the preparation process of $Cr(OH)_3$ which has a similar value (577.93 eV), however, on inspection of survey scan results (only 2.3% Cl detected) this is unlikely. The binding energy value also indicates that the drying method used for the preparation of this standard did not have the effect of transforming $Cr(OH)_3$ to Cr_2O_3. (see table 3). It is possible that the chemical structure of $Cr(OH)_3$ may also be present as $Cr(OH)_3.3H_2O$.

It is important to note that a $2p_{1/2}$ satellite can be observed on the spectra. The corresponding $2p_{3/2}$ satellite may be overlapped by the Cr $2p_{1/2}$ profile.

A high resolution $Cr(OH)_3$ O1s spectrum is provided in figure 3b. The binding energy value of the major peak (531.91 eV) is at least 1 eV higher than that of Cr_2O_3 and CrO_3 (table 4). The peak shoulders are observed either side of the major peak profile. Their peak maximum positions of 533.07 and 530.39 eV could be representative of water containing species as well as oxygen associated with other forms of chromium such as Cr_2O_3 or CrO_3.

Table 3 – $Cr2p_{3/2}$ curve fitted peak maximum BE, FWHM and area percentage values. All BE values are charge corrected to C1s at 285 eV

Standard	Peak 1	FWHM	%	Peak 2	FWHM	%	Peak 3	FWHM	%	Peak 4	FWHM	%
Cr_2O_3	575.83	0.8	24.59	577.03	1.55	52.16	578.56	1.74	17.02	579.97	2.4	6.24
CrO_3	578.30	2.70	15.40	579.96	1.33	69.59	581.06	1.28	15.01			
$Cr(OH)_3$	577.79	2.44	100									

Table 4 – $O1s_{1/2}$ curve fitted peak maximum BE, FWHM and area percentage values. All BE values are charge corrected to C1s at 285 eV

Standard	O1s (left peak) (eV)	FHWM	Area %	O1s (main) (eV)	FHWM	Area %	O1s (right peak) (eV)	FHWM	Area %
$Cr(OH)_3$	533.07	2.15	17.6	531.91	1.54	75.4	530.39	1.30	6.9
CrO_3	531.81	1.58	30.4	530.74	1.31	69.6			0.0
Cr_2O_3	531.56	2.79	42.9	530.45	0.93	57.1			0.0

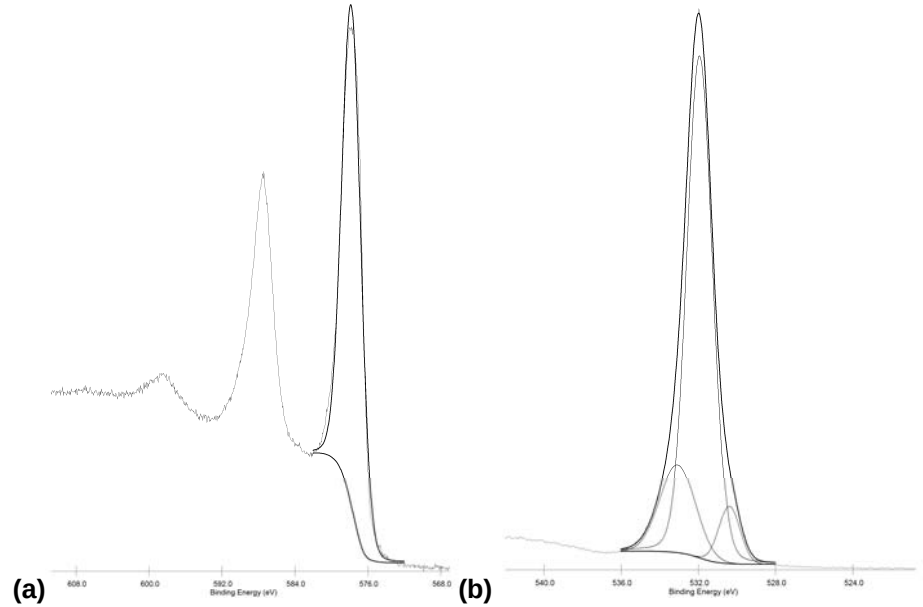

Figure 3 - High resolution Cr2p (a) 01s (b) spectra of $Cr(OH)_3$ compound

Chromium conversion coating survey scan data

Survey scan results of hexavalent and trivalent CCC are provided in table 5. Distinct differences that occur between the two coatings are a higher percentage of Zn detected for trivalent CCC and the detection of S for hexavalent CCC.

Table 5 – Survey scan data of hexavalent and trivalent chromium conversion coatings

	Atomic %					
	C1s	**O1s**	**Cr2p**	**Zn2p**	**S2p**	**Cl2p**
Hexavalent CCC	21.6	59.6	15.5	0.9	2.4	0.0
Trivalent CCC	13.8	56.8	8.2	21.2	0.0	0.0

Hexavalent & trivalent chromium conversion coating

Hexavalent and trivalent CCC Cr2p spectra are provided in figures 4a & b. A marked difference between the two profiles is a shoulder present on the $2p_{3/2}$ peak for hexavalent CCC. Curve fitting of the spectrum with CrO_3, Cr_2O_3 and $Cr(OH)_3$ reference peaks indicates that the shoulder region is associated with CrO_3 or of a similar oxidation state species (table 6.1 and 6.2). Curve fitting data also indicates that trivalent CCC are largely composed of chromium as Cr_2O_3 as opposed to $Cr(OH)_3$ which is the case for hexavalent CCC (table 6.1 and 6.2). It is also important to note that the $2p_{1/2}$ peak area for trivalent CCC is similar to that of its $2p_{3/2}$ peak in size and shape. This phenomenon does not appear to be reported for trivalent CCC XPS Cr2p spectra [15,16]. This is possibly due to an unusual loss of structure on the $2p_{3/2}$ peak or an effect of rising background signals.

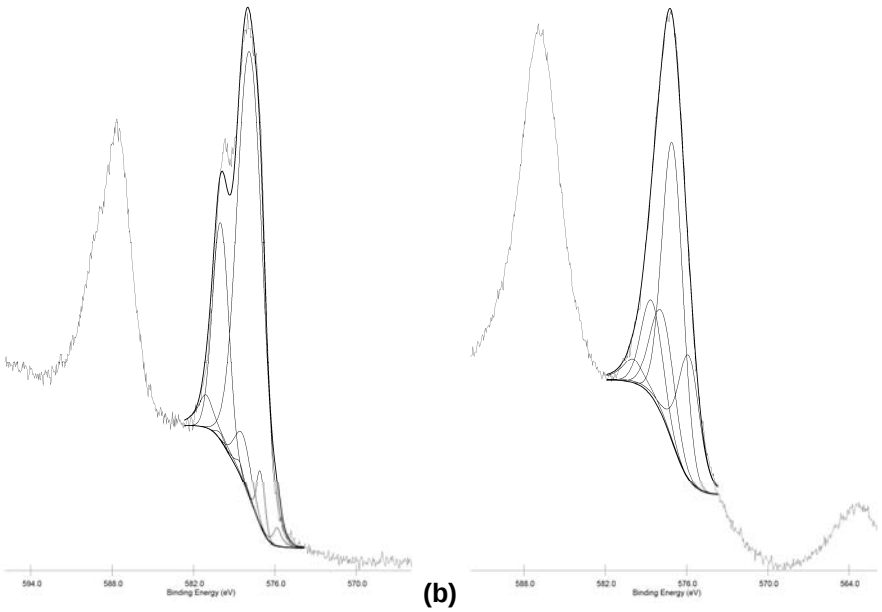

Figure 4 - High resolution Cr2p hexavalent (a) and trivalent (b) chromium conversion coating spectra

Oxygen 1s spectra for the coatings are provided in figures 5a & b. The hexavalent CCC differs to that of the trivalent CCC profile in that shoulders can be observed either side of the main peak maximum as opposed to just one side. Curve fitting of the hexavalent CCC O1s spectrum provides similar peak maximum binding energy positions to that of $Cr(OH)_3$ O1s (tables 4 & 7). The $Cr(OH)_3$ sample spectrum also exhibits shoulders either side of the main peak maximum. Curve fitting of the trivalent CCC O1s spectrum appears to show that the main oxygen peak maximum binding

energy is similar to that of Cr_2O_3 O1s shoulder peak maximum binding energy value (tables 4 & 7). Thus both data from Cr and O peak envelopes are consistent.

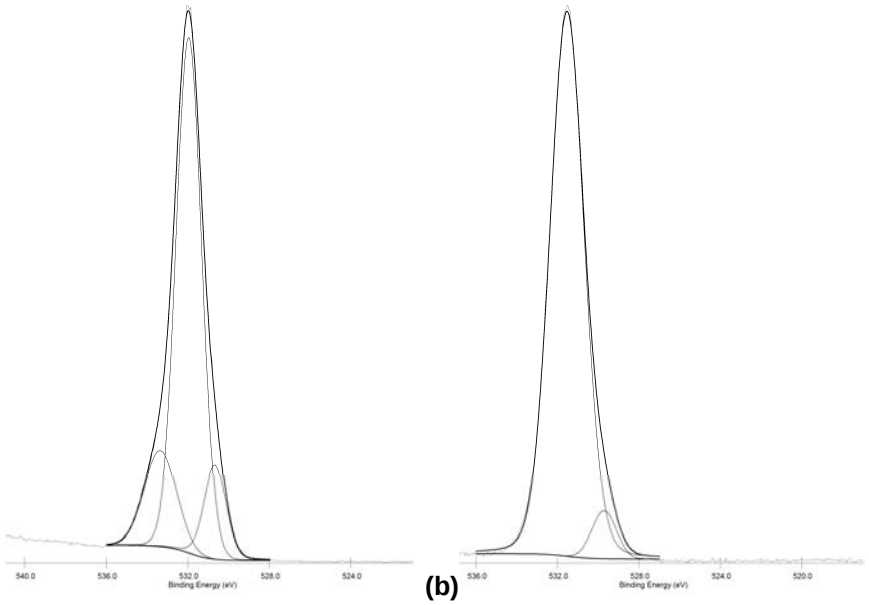

Figure 5 - High resolution O1s hexavalent (a) and trivalent (b) chromium conversion coating spectra

Hexavalent conversion coating depth profile

Hexavalent CCC Cr2p spectra taken at 10° and 30° TOA are provided in figure 6a & b. The spectra profiles, like that of the hexavalent CCC Cr2p spectrum taken at 90° TOA, exhibit a shoulder region off the main peak maximum. Curve fitting once again indicates that the shoulder region is associated with CrO_3 or of a similar chromium oxidation state species (table 6.1). Curve fitting data also appears to show that at 10° and 30° TOA a slightly higher CrO_3 content and a reduction of Cr_2O_3 content is produced in comparison to the 90° TOA. Variation between 10° and 30° TOA appears to be minimal.

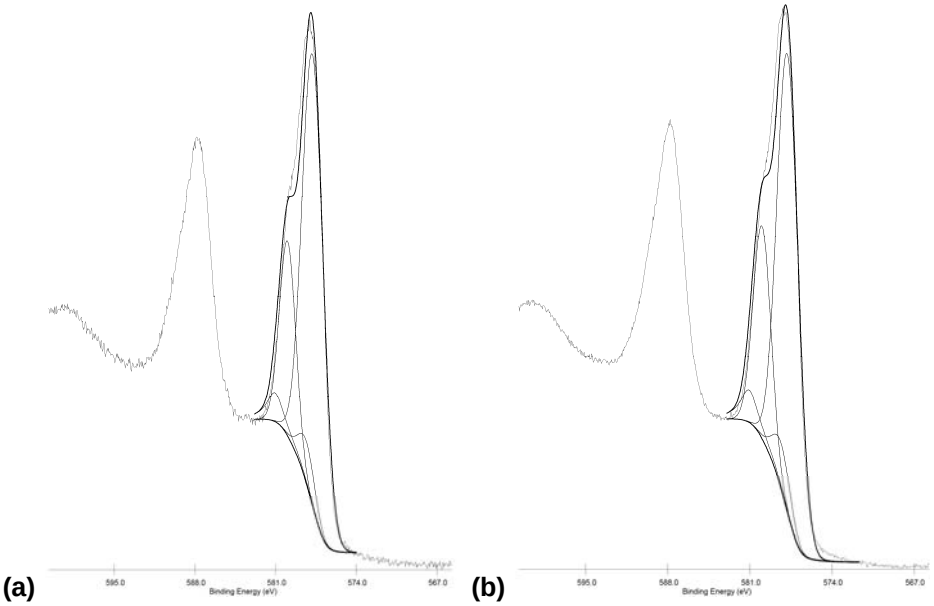

Figure 6 - High resolution Cr2p hexavalent chromium conversion coating spectra taken at 10° (a) and 30° (b) TOA

An oxygen 1s spectrum of a hexavalent CCC taken at 10° take off angle is provided in figure 7. The profile is similar to that of the hexavalent CCC 90° TOA spectrum profile in which shoulders either side of the main peak maximum are present. Curve fitting of their respective binding energy positions and area % are also similar (see table 7).

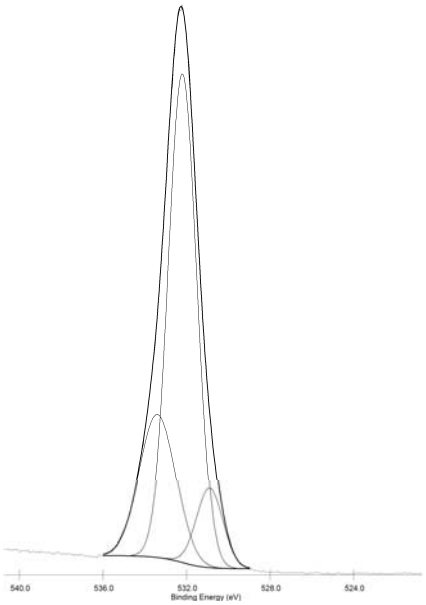

Figure 7 - High resolution O1s hexavalent chromium conversion coating spectrum taken at 10° TOA

Table 6.1 – Summary of relative peak area percentages for $Cr2p_{3/2}$ curve fitted coating data presented in table 6.2

Sample	Cr_2O_3 (%)	$Cr(OH)_3$ (%)	CrO_3 (%)
Hexvalent CCC	4.93	65.81	29.26
Trivalent CCC	83.18	16.82	0.00
Hexvalent CCC 10° TOA	0.00	67.44	32.56
Hexvalent CCC 30° TOA	0.00	64.19	35.81

Table 6.2 – $Cr2p_{3/2}$ curve fitted peak maximum BE, FWHM and area % values of chromium coating using Cr_2O_3, $Cr(OH)_3$ and CrO_3 as reference compounds. All binding energy values are charge corrected to C1s at 285 eV.

Sample	Peak 1	Area	FHWM	Peak 2	Area	FHWM	Peak 3	Area	FHWM	Peak 4	Area	FHWM	Cr_2O_3 (Area %)
Hexavalent CCC	575.83	333	0.69	577.03	709	0.69	578.56	234	0.69	579.97	85	0.69	4.93
Trivalent CCC	575.83	12109	1.83	577.03	25763	1.83	578.56	8502	1.83	579.97	3092	1.83	83.18
Hexavalent CCC 10° TOA	575.83	0.05	0.23	577.03	0.10	0.23	578.56	0.03	0.23	579.97	0.01	0.23	0.00
Hexavalent CCC 30° TOA	575.83	0.00	0.00	577.03	0.00	0.00	578.56	0.00	0.00	579.97	0.00	0.00	0.00

Table 6.2 – continued

Sample	Peak 5	FHWM	Area	Peak 6	FHWM	Area	Peak 7	FHWM	Area	CrO_3 (Area %)	Peak 8	Area	FHWM	$Cr(OH)_3$ (Area %)
Hexavlent CCC	581.06	1.41	1243	579.96	1.41	5618	578.30	1.41	1212	29.26	577.79	18160	2.21	65.81
Trivalent CCC	581.06	0.00	0.00	579.96	0.00	0.00	578.30	0.00	0.00	0.00	577.79	10002	2.04	16.82
Hexvalent CCC 10° TOA	581.06	1.67	3514	579.96	1.67	15881	578.30	1.67	3426	32.56	577.79	47274	2.14	67.44
Hexvalent CCC 30° TOA	581.06	1.78	11557	579.96	1.78	52225	578.30	1.78	11265	35.81	577.79	134510	2.13	64.19

Table 7 – Hexavalent and trivalent CCC $O1s_{1/2}$ curve fitted peak maximum BE, FWHM and area % values. All binding energy values are charge corrected to C1s at 285 eV

Sample	O1s BE (left peak (eV)	FHWM	Area %	O1s BE (main) (eV)	FHWM	Area %	O1s BE (right peak) (eV)	FHWM	Area %
Hexavalent CCC	533.23	1.98	19.6	531.92	1.44	67.5	530.69	1.29	12.9
Hexavalent CCC (flood gun)	533.33	2.01	21.7	532.10	1.46	64.9	530.85	1.35	13.4
Trivalent CCC			0.0	531.53	1.96	94.6	529.72	1.36	5.4
Hexavalent CCC 10° TOA	533.30	2.05	25.4	532.14	1.58	62.7	530.88	1.54	11.9

Discussion

Film formation process for hexavalent CCC

In order to elucidate the film formation process of hexavalent CCCs it is important to identify the role of additives during the solution preparation and coating processing stage. During the coating processing stage in which the zinc electrodeposited steel is immersed into the solution a series of anodic/cathodic reactions are likely to take place. Firstly, the acidic nature of the solution initiates zinc dissolution and as a consequence certain additives are likely to be reduced forming insoluble compounds which form part of the coating [17]. These reactions are listed in table 8. Certainly some of these reactions are more favourable than others and may be identified by reference to the curve fitted hexavalent CCC Cr2p data (tables 6.1 and 6.2), which indicates the formation of $Cr(OH)_3$. However, for this reaction to take place the film formation process would have to be controlled by the dissolution rate of zinc in order to achieve the reduction of dichromate ions. XPS survey scan results (table 5) has shown that the incorporated zinc content to be minimal as AES depth profiling indicated by Chapaneri et al [18], with levels only increasing at the zinc electrodeposit interface or if the coating is very thin [18]. Such a situation whereby zinc levels are low through the coating indicates that the conversion coating growth mechanism may not be entirely an electrochemical dissolution / precipitation process as referred to by previous researchers [1,19-21]. It may already be that sufficient zinc has undergone dissolution for the reduction of Cr(VI). An alternative film formation mechanism could be based on a 'sol-gel' reaction following zinc dissolution [22]. This could also confirm why $Cr(OH)_3$ appears to form the basis of the coating.

Table 8 – Potential redox reactions between substrate and passivation solution, after M.P. Gigandet et al [17]

	Equations
Oxidation reactions	$Zn \leftrightarrow Zn^{2+}(aq) + 2e^{-}(aq)$
Reduction reactions	$2H^{+}(aq) + 2e^{-}(aq) \leftrightarrow H_2(g)$ $Cr_2O_7^{2-}(aq) + 14H^{+}(aq) + 6e^{-} \leftrightarrow 2Cr^{3+}(aq) + 7H_2O(l)$
Complex reactions	$Cr^{3+}(aq) + 6H_2O(l) \rightarrow [Cr(H_2O)_6]^{3+}(aq)$
Insoluble Reduction reactions	$[Cr(H_2O)_6]^{3+}(aq) + 3H_2O(l) \leftrightarrow [Cr(H_2O)_3(OH)_3](s) + 3H_3O^{+}(aq)$ $Cr_2O_7^{2-}(aq) + 2H^{+}(aq) \leftrightarrow 2CrO_3(s) + H_2O(l)$ $CrO_4^{2-}(aq) + Zn^{2+} \leftrightarrow ZnCrO_4(s)$ $Cr_2O_7^{2-}(aq) + Zn^{2+} \leftrightarrow ZnCr_2O_7(s)$ $Cr_2O_7^{2-}(aq) + 8H^{+}(aq) + 6e^{-} \leftrightarrow Cr_2O_3(s) + 4H_2O(l)$ $2HCrO_4^{-}(aq) + 8H^{+}(aq) + 6e^{-} \rightarrow 2Cr(OH)_3(s) + 2H_2O(l)$ $Zn + 2H_2O \rightarrow Zn(OH)_2(s) + H_2(g)$ $Zn + H_2O \rightarrow ZnO(s) + H_2(g)$

It is important to note that not all of the chromium content relies upon the dissolution of zinc in order to form part of the coating. CrO_3 (~29%) has been established from curve fitted hexavalent CCC data with its percentage value increasing marginally when conducting lower XPS TOA measurements (table 6.1). Other similar oxidation state species may also be incorporated in small quantity such as soluble $Cr_2O_7^{2-}$ or CrO_4^{2-} ions or associated zinc compounds ($ZnCrO_4$, $ZnCr_2O_7$).

The effect of nitric and sulphuric acids on film formation of hexavalent CCC

The role of sulphuric and nitric acid is thought to provide a low pH environment for zinc dissolution in the passivation process. The incorporation of sulphur within the hexavalent CCC exhibited in XPS survey scan data (table 5), is possibly as an absorbed sulphate residue e.g. SO_4^- or HSO_4^-. Formation of a chromium-sulphur containing compound is debatable due to the low elemental contents detected from XPS survey scans (table 5). AES data [18] appears to indicate that sulphur is present only in the surface regions of the coating. The absence of nitrogen in the XPS data may indicate that nitric acid promotes Zn^{2+} but doesn't become involved in the coating.

Film formation process of trivalent CCC

The film formation process for trivalent chromium CCC is different to the mechanism by which a hexavalent CCC is formed. The addition of complexants, organic acids and other metal ions would all contribute. XPS survey scan results have demonstrated a high yield of zinc within the coating surface and this could be related to the acidic nature of the process solution. Curve fitting has demonstrated that the chromium oxidation state is composed solely of Cr(III) compounds, with Cr_2O_3 formation being more favourable than that of $Cr(OH)_3$. Corresponding to this, to a certain degree, is that the O1s curve fitted data exhibits a shoulder which has a similar peak binding energy to that of a shoulder present on the Cr_2O_3 curve (531.5 to 531.56 eV). The mechanism by which trivalent chromium compounds are formed could be via complexants / ligand substitution reactions, addition of oxidising agents and metal ion catalysts. Excess zinc incorporated within the coating would be present as $Zn(OH)_2$ or ZnO with some possibly even associated with chromium.

Conclusion

Analysis and curve fitting of monochromatic AlKα XPS data on chromium compounds and chromium conversion coatings on zinc electrodeposited steel has revealed the following:

1) $Cr2p_{3/2}$ peak multiplet splitting was observed for Cr_2O_3 compound. Cr2p satellite emissions were also observed for this compound as well as for $Cr(OH)_3$. No such features were observed for CrO_3.
2) Hexavalent CCC $Cr2p_{3/2}$ peak profile exhibited an additional overlapping chemical shoulder representative of a Cr(VI) state species in comparison to trivalent CCC. Curve fitting of $Cr2p_{3/2}$ using parameters established from chromium compounds revealed that the trivalent CCC was largely composed of Cr_2O_3 as opposed to $Cr(OH)_3$. Hexavalent CCC was largely composed of $Cr(OH)_3$ with some Cr_2O_3. These finding are also complemented by O1s analysis. Survey scan results for the relative zinc content in hexavalent and trivalent CCCs appears to indicate that the film formation mechanisms are different.
3) Trivalent CCC Cr2p spectrum was found to exhibit unusually similar peak area profiles for $2p_{3/2}$ and $2p_{1/2}$ envelopes.
4) Evaluation of curve fitted hexavalent CCC $2p_{3/2}$ peak profiles at lower X-ray beam take off angles (10° and 30°) for more surface specific information, indicates a slightly higher Cr(VI) to Cr(III) content. Data differences between 10° and 30° TOA appears to be minimal.

Outlook

In future studies hexavalent and trivalent CCC film chemistry will be characterised using XPS following exposure to heat treatment and a corrosive environment. The film chemistry will then be compared to the untreated film chemistry elucidated in this paper.

Acknowledgements

The Engineering and Physical Sciences Research Council (EPSRC) is acknowledged for financial support of NCESS via grants GR/S14252/01 and EP/E025722/1. MacDermid plc is also acknowledged for financial support of this project.

References

[1] Van de Leest, R. E., Trans. Inst. Met. Finish. 56 (1978) 51.

[2] G. Raichevsky, V. Ivanova, S. Vitkova, M. Nikolova, Surf Coat Technol 82 (3) (1996) 239.

[3] G. Bikulcius, A. Rucinskiene, E. Matulionis, A. Sudavicius, Surface and Coatings Technology 187 (2-3) (2004) 388.

[4] R. Ramanauskas, Gudaviciu over-bar te, L., L. Diaz-Ballote, P. Bartolo-Perez, P. Quintana, Surface and Coatings Technology v 140, n 2 (May 30, 2001) p 109-115.

[5] G.M. Treacy and G.D. Wilcox, Appl. Surf. Sci. 157 (1) (2000) 7.

[6] X. Zhang, W.G. Sloof, A. Hovestad, E.P.M. van Westing, H. Terryn, J.H.W. de Wit, Surface and Coatings Technology 197 (2-3) (2005) 168.

[7] M.C. Biesinger, C. Brown, J.R. Mycroft, R.D. Davidson, N.S. McIntyre, Surf Interface Anal 36 (12) (2004) 1550.

[8] E. Unveren, E. Kemnitz, S. Hutton, A. Lippitz, W.E.S. Unger, Surf Interface Anal 36 (1) (2004) 92.

[9] XPS Survey scan,

[10] Kwok. R.W.M., 4.1 (2000)

[11] Ilton ES, deJong WA, Bagus PS, Phys. Rev. B 125106 (2003)

[12] Charles. D., Wagner.D.C, Naumkin. A., Kraut-Vass. A., Allison. J., Powell. C, Rumble .J., NIST X-ray Photoelectron Spectroscopy Database, http://srdata.nist.gov/xps/, 2003.

[13] D. Chidambaram, G.P. Halada, C.R. Clayton, Appl. Surf. Sci. 181 (3-4) (2001) 283.

[14] S.V. Kagwade, C.R. Clayton, G.P. Halada, Surf Interface Anal 31 (6) (2001) 442.

[15] X. Zhang, van den Bos, C., W.G. Sloof, A. Hovestad, H. Terryn, J.H.W. de Wit, Surface and Coatings Technology v 199, n 1 (Sep 1, 2005) p 92-104.

[16] K. Cho, V. Shankar Rao, H. Kwon, Electrochim. Acta 52 (13) (2007) 4449.

[17] M.P. Gigandet, J. Faucheu, M. Tachez, Surf Coat Technol 89 (3) (1997) 285.

[18] Chapaneri R., Critchlow G.W., Smith R.G., Sutherland I., Wilcox G.D., Chojnicki A., Pearson T., Rowan A.J., An analytical investigation into micro-cracking of hexavalent chromium based conversion coatings, submitted.

[19] M.W. Kendig, A.J. Davenport, H.S. Isaacs, Corros. Sci. 34 (1) (1993) 41.

[20] H.A. Katzman, G.M. Malouf, R. Bauer, G.W. Stupian, Applications of Surface Science 2 (3) (1979) 416.

[21] P. Campestrini, G. Goeminne, H. Terryn, J. Vereecken, J.H.W. De Wit, J. Electrochem. Soc. 151 (2) (2004) 59.

[22] J.H. Osborne, Progress in Organic Coatings 41 (4) (2001) 280.